Examination of change in arterial wall viscoelasticity by internal pressure in ultrasonic measurement

Saki Suzuki[1‡], Shohei Mori[2], Masumi Iwai-Takano[3,4,1], Mototaka Arakawa[1,2], and Hiroshi Kanai[2,1] ([1]Grad. School Biomed. Eng., Tohoku Univ.; [2]Grad. School Biomed. Eng., Tohoku Univ.; [3]Dept. Epidemiol., Fukushima Med. Univ.; [4]Dept. Cardiovasc. Surg., Fukushima Med. Univ.)

1. Introduction

We have been proposing an ultrasonic method of estimating the elasticity of blood vessels for early detection of arteriosclerosis by measuring the thickness change of the vessel wall caused by pulsation [1]. In our previous study, we confirmed that the ultrasonic measurement can estimate the elasticity as accurately as the laser measurement through a phantom experiment [2]. However, because the experimental system in the previous study could not apply high internal pressure, the previous study simulated only the pulse pressure conditions in *in vivo* and did not simulate the systolic and diastolic blood pressures and the blood flow rate. Since the relationship between the internal pressure and the vessel diameter is nonlinear [3], the viscoelasticity of blood vessels could depend on the steady internal pressure. Clarifying the relationship between blood pressure and the viscoelasticity of blood vessels may help predict hypertension and atherosclerosis. In the present study, we constructed an experimental system that can apply high internal pressure and simulates the blood pressure and blood flow conditions in *in vivo* and investigated the effect of internal pressure on the estimation of viscoelastic properties by the phantom experiment.

2. Principle and method

2.1 Viscoelasticity estimation method

Assuming that the arterial wall is isotropic and elastically incompressible, and expansion or contraction does not occur along the longitudinal direction, the relationship between the strain $\varepsilon_r(t) = \Delta h(t)/h_0$ caused by the wall thickness change $\Delta h(t)$ and the incremental internal pressure $\Delta p(t)$ can be expressed by the Voigt model as follows [1]:

$$-\frac{3}{8}\left(1+\frac{2r_0}{h_0}\right)\Delta p(t) = E\varepsilon_{\mathrm{r}}(t) + \eta\dot{\varepsilon}_{\mathrm{r}}(t), \qquad (1)$$

where r_0 and h_0 are the initial inner radius and thickness of the vessel, respectively, and E and η are the elastic and viscous moduli of the arterial wall, respectively. The change in the arterial wall thickness $\Delta h(t)$ is calculated by integrating the velocity waveforms obtained by the phased-tracking method [4]. The initial thickness h_0 and the initial inner radius r_0 were measured by observing the ultrasonic B-mode image. The elasticity E and viscosity η were estimated to minimize the squared error between the measured incremental internal pressure $\Delta p_{\mathrm{meas}}(t)$ and the model $\Delta p_{\mathrm{model}}(t)$ in Eq. (1).

2.2 Construction of experimental system

In our previous study [1], water was circulated by a pulsating pump (EC-8, Fuyo, Japan) in a tube through an open tank; therefore, it is difficult to simulate the high steady internal pressure in *in vivo*. In the present study, we constructed a new experimental system where water was circulated in the closed circulation path as shown in **Fig. 1**. The high steady pressure was applied by the water column without changing the flow rate. To stably measure the pressure waveform, the air in the circulation path must be drained out and replaced with water using valves (I) and (II).

2.3 Experimental method

In the ultrasound measurement, a linear probe with a central frequency of 7.5 MHz was connected to an ultrasonic diagnostic device (SSD-6500, Aloka, Japan). The sampling frequency, beam spacing, and frame rate were 40 MHz, 150 μm, and 286 Hz, respectively. To simulate the carotid artery, we used a silicone rubber tube with an ASKER-C hardness of 10°, an external diameter of 9 mm, an inner diameter

E-mail: saki.suzuki.q6@dc.tohoku.ac.jp

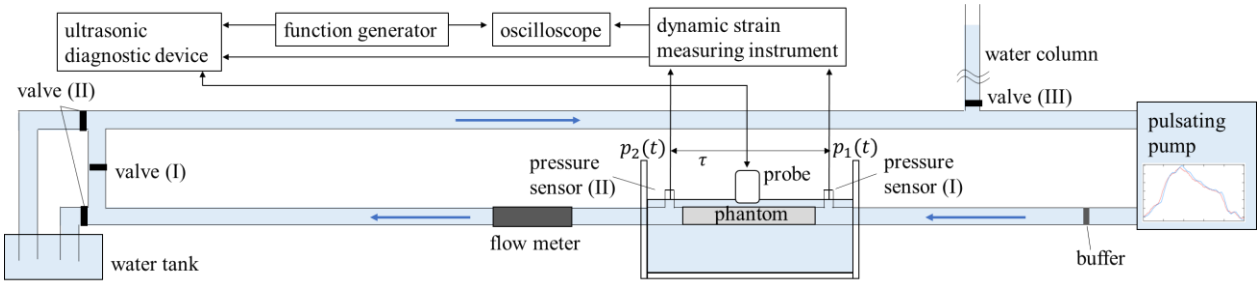

Fig. 1. Experimental system.

of 7 mm, and a wall thickness of 1 mm (nominal values). The pulsation rate was set to 70 times/min.

The internal pressures $p_1(t)$ and $p_2(t)$ were measured by pressure sensors (I) and (II) (PS-1KC, Kyowa, Japan), positioned upstream and downstream to the phantom, respectively. The thickness change of the posterior wall was measured by ultrasound at an equidistant position from the two pressure sensors. The delay time τ between the two pressure waveforms was determined using the cross-correlation function, and each pressure waveform was shifted by $\tau/2$ to compensate for the delay time.

To simulate the *in vivo* blood pressure conditions, the steady-state water column height was set to 130 cm so that the maximum and minimum water pressures became 120 mmHg (160 $\mathrm{cmH_2O}$) and 75 mmHg (100 $\mathrm{cmH_2O}$), respectively. As a comparison, the several heights of the water column, 0, 30, 60, and 100 cm, were also examined. The pump output was set to be that the water flow rate became 600 mL/min to simulate the carotid blood flow rate. The flow rate per pulsation was measured by integrating the instantaneous flow rate obtained by the ultrasound-based flow meter (FD-XS20, Keyence, Japan).

3. Results and discussion

Figure 2(a) shows the B-mode image (at minimum pressure) when the steady pressure due to the water column was 130 $\mathrm{cm\,H_2O}$ (*in vivo* condition). The beam shown by the red line was analyzed to measure the thickness change of the posterior wall. Figure 2(b) shows the internal pressure waveforms $p_1(t)$ for four circulation cycles when the steady pressures due to the water column were 130, 100, 60, 30, and 0 $\mathrm{cmH_2O}$. The maximum and minimum pressures increased as the water column was heightened. Figure 2(c) shows the incremental strain waveform $\varepsilon(t)$. The strain increased for water column height from 0 to 60 cm and decreased from 60 to 130 cm. Figure 2 (d) shows the hysteresis loops between the internal pressure $p_1(t)$ and the incremental strain $\varepsilon(t)$. When the pressure due to the water column was 100 $\mathrm{cmH_2O}$ and over, the hysteresis loops were nonlinear, that is, the slope increased at higher pressures. One of the considerable reasons is that the viscoelasticity depends on internal pressure, so the higher the internal pressure, the larger the elasticity and the smaller the strain.

The means and standard deviations of the elastic and viscous moduli for the four circulation cycles are summarized in **Table 1**. The viscoelasticity values were close from 0 to 60 $\mathrm{cmH_2O}$, but they were estimated to be higher at 100 and 130 $\mathrm{cm\,H_2O}$. This suggests that the viscoelasticity of the silicone rubber phantom depends on the steady internal pressure.

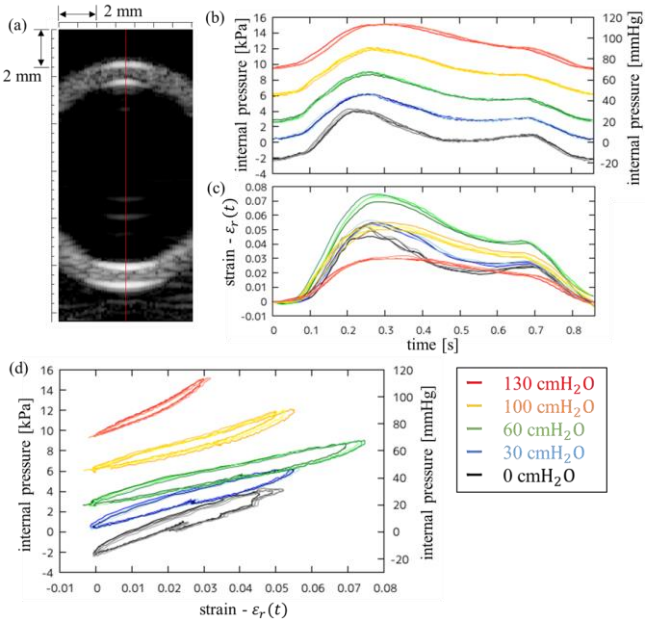

Fig. 2. (a) A B-mode image of the silicone rubber phantom at the minimum pressure when the steady pressure due to the water column was 130 $\mathrm{cm\,H_2O}$. (b) The internal pressures $p(t)$, (c) the incremental strains $\varepsilon(t)$, and (d) the hysteresis loops between them for four circulation cycles.

4. Conclusion

In this study, we constructed the experimental system that simulates blood pressure and blood flow conditions in *in vivo* and confirmed that viscoelasticity changes significantly depending on maximum and minimum pressures. In the future, we will investigate the effects of changes in maximum and minimum blood pressures on viscoelasticity in *in vivo* measurements.

Acknowledgment

This work was supported by 21H03835.

References

1. H. Kanai, *et al.*: Circulation, **107**, (2003) 3018.
2. S. Akiyama, *et al.*: Jpn. J. Appl. Phys. **60**, (2021) SDDA07.
3. P. B. Dobrin: Physiol. Rev., **58**, (1978) 397.
4. H. Kanai, *et al.*: IEEE Trans. Ultrason. Ferroelectr. Freq. Control **43**, (1996) 791.

Table 1. The means and standard deviations of the elastic and viscous moduli of the silicone rubber phantom for the four circulation cycles.

Pressure by water column [$\mathrm{cmH_2O}$]	130	100	60	30	0
Elasticity E [kPa]	985±6	493±5	295±8	318±4	360±4
Viscosity η [kPa·s]	13.8±2.3	10.1±1.3	7.8±0.5	7.7±0.6	6.2±0.8